LM-04K040
June 9, 2004

Antimony Based III-V Thermophotovoltaic Devices

C.A. Wang

NOTICE

This report was prepared as an account of work sponsored by the United States Government. Neither the United States, nor the United States Department of Energy, nor any of their employees, nor any of their contractors, subcontractors, or their employees, makes any warranty, express or implied, or assumes any legal liability or responsibility for the accuracy, completeness or usefulness of any information, apparatus, product or process disclosed, or represents that its use would not infringe privately owned rights.

The Sixth Conference on Thermophotovoltaic Generation of Electricity
14-16 June 2004 Freiburg, Germany
Invited Paper

Antimony-Based III-V Thermophotovoltaic Materials and Devices

C.A. Wang

Lincoln Laboratory, Massachusetts Institute of Technology, Lexington, MA 02420-9108

ABSTRACT

Antimony-based III-V thermophotovoltaic (TPV) cells are attractive converters for systems with low radiator temperature around 1100 to 1700 K, since these cells potentially can be spectrally matched to the thermal source. Cells under development include GaSb and the lattice-matched GaInAsSb/GaSb and InPAsSb/InAs quaternary systems. GaSb cell technology is the most mature, owing in part to the relative ease in preparation of the binary alloy compared to quaternary GaInAsSb and InPAsSb alloys. Device performance of 0.7-eV GaSb cells exceeds 90% of the practical limit. GaInAsSb TPV cells have been the primary focus of recent research, and cells with energy gap E_g ranging from ~0.6 to 0.49 eV have been demonstrated. Quantum efficiency and fill factor approach theoretical limits. Open-circuit voltage factor is as high as 87% of the practical limit for the higher-E_g cells, but degrades to below 80% with decreasing E_g of the alloy, which might be due to Auger recombination. InPAsSb cells are the least studied, and a cell with E_g = 0.45-eV has extended spectral response out to 4.3 µm. This paper briefly reviews the main contributions that have been made for antimonide-based TPV cells, and suggests additional studies for further performance enhancements.

*This work was sponsored by the Department of Energy under AF Contract No. F19628-00-C-0002. The opinions, interpretations, conclusions and recommendations are those of the author and are not necessarily endorsed by the United States Government.

1. INTRODUCTION

Thermophotovoltaic (TPV) systems generate electricity from thermal radiation using photovoltaic cells. Various types of TPV cells were used in recent TPV demonstrations, including those based on Si or III-V semiconductors with lower energy gap E_g such as GaSb, InGaAs or GaInAsSb [1]. Based on recent modeling of TPV generators, a system with a black-body thermal source heated to temperatures between 800 and 1700 °C might be optimized for efficiency and power density with diodes of energy gap E_g in the range 0.4 to 0.7 eV [2,3]. The type of diode selected for the TPV generator, however, is not necessarily straightforward, and depends on several factors including end application, system efficiency, power density, engineering feasibility, and overall cost. For example, a TPV system was designed for use with Si cells since these are readily available at low cost [4]. The reported efficiency and power density with a selective emitter at 1450 °C was 2.4% and ~1 W/cm^2, respectively. The performance is limited in part by the small fraction of photons that can be converted by 1.1-eV Si cells.

Semiconductor materials with lower E_g in the range 0.4 to 0.7 eV can utilize a larger fraction of the power from the thermal radiator, and therefore, several alternatives to Si cells are being developed [5]. Figure 1 shows the E_g versus lattice constant of the main materials being developed. GaSb and the $In_{0.53}Ga_{0.47}As$ ternary alloy, which is lattice matched to InP, have E_g around 0.7 eV. Alloys with lower E_g include higher In containing InGaAs alloys, which are mismatched to InP, and GaInAsSb and InPAsSb quaternary alloys, which can be lattice-matched to either GaSb or InAs. GaInAsSb alloys have E_g ranging from 0.7 for GaSb to 0.3 eV for InAsSb, although the practical range is 0.5 to 0.7, as will be discusses further, while InPAsSb can be used for cells with E_g from 0.35 to 0.5 eV.

GaSb cells are inherently more straightforward to fabricate compared to ternary and quaternary diodes, and thus they are obviously more cost effective for production of TPV generators, albeit for systems that operate at the higher end of thermal source temperatures. A TPV system using GaSb cells reported efficiency as high as 10.9% and power density of ~0.8 W/cm^2 for a radiator temperature of 1150 °C [6]. For systems designed to operate at lower radiator temperatures, lattice-mismatched InGaAs ternary and GaInAsSb quaternary TPV cells are being developed. 0.6-eV InGaAs cells were used with a radiator at 1039 °C and a heat to electric conversion efficiency of 23.6% and power density of 0.79 W/cm^2 were recently reported [7]. At a lower radiator temperature of 954 °C, 0.53-eV GaInAsSb cells were used and efficiency of 17.5% and power density of 0.8 W/cm^2 were reported [8,9]. Although record efficiencies are achieved for 0.6-eV InGaAs cells, which may be related in part to their longer development period and the use of a back-surface reflector, the lower E_g of GaInAsSb cells can potentially yield higher power densities. While the reported system efficiencies are also dependent on spectral control of below bandgap photons, these comparisons are nevertheless illustrative of the advantage of using the cells with lower E_g compared to Si.

Sb-based TPV cells offer the potential for the largest range of E_g compared to any other semiconductor materials system. A wide variety of cells have been reported, and Figure 2 shows that the spectral response of GaSb, GaInAsSb, and InPAsSb TPV cells can cover a broad range from 1.7 to 4.3 µm. The quantum efficiencies have each been normalized to unity for ease of comparison of the cutoff wavelengths and do not reflect the absolute values of spectral response. This paper reviews major achievements made in Sb-based TPV cells. A separate review of InGaAs/InP is provided in another paper in these proceedings. Recent work on the more mature GaSb cells is briefly summarized first, followed by the more limited efforts on InAsPSb. A

significant portion of the paper discusses the preparation and performance of GaInAsSb materials and TPV cells, as this system has shown significant promise for TPV generators that are designed to operate with low radiator temperatures [10].

2. GaSb TPV CELLS

GaSb solar cells were first reported in 1980, and were of interest as a low E_g cell for tandem solar cells [11]. While initial demonstrations used epitaxial structures, a simple Zn-diffusion process was developed to form the p-n junction, and GaSb cells were mechanically stacked in tandem with GaAs solar cells to enhance conversion efficiency in [12]. It was recognized early on that these 0.7-eV cells could be advantageous for TPV applications, and in 1990, a design analysis of a radioisotope TPV system with GaSb cells was made [13]. This study outlined the benefits of the low E_g of GaSb, as well as the importance of a reflective back contact to improve efficiency. The development of GaSb cells for tandem solar cells played a key role in the rapid progress in of TPV generators, and the first GaSb TPV system was reported at the 1st NREL Conference on Thermophotovoltaic Generation of Electricity held in 1994 [14]. Since then, several groups have worked on process optimization and modeling of GaSb cells [15-21]. These cells have now reached a high level of maturity and are commercially available. There was a strong interest in GaSb cells for TPV systems, and numerous groups reported systems based on GaSb cells at the 4th NREL Conference on Thermphotovoltaic Generation of Electricity held in 1998 [22].

2.1 Diffused-Junction GaSb Cells

GaSb cells can be fabricated by Zn diffusion of bulk grown n-type GaSb wafers, which makes for a much simpler and lower cost process compared to ternary and quaternary cells that

typically involve an epitaxial process. A detailed study of the diffusion process and cell operation demonstrated the impact of the Zn profile on TPV cell performance [15-17]. Zn diffusion is performed in a 'pseudo-closed' box that contains elemental Zn and Sb as sources for vapor diffusion and the n-type GaSb wafers. The Zn-doping profile was studied for various temperature and time conditions, and precise control of p-n junction depth was achieved by a two-step Zn-diffusion process combined with anodic oxidation and selective etching. Profiles were optimized to establish internal electric fields of the p-n junction in order to maximize collection of minority carriers. Furthermore, it was noted that the Zn profile near the surface could be formed to create a high electric field of ~8kV/cm to limit minority-carrier diffusion to the surface, thus reducing surface recombination velocity. Therefore, no surface passivation layer or subsequent surface treatment was needed. The performance of GaSb cells can be very high, and internal quantum efficiency (IQE) slightly exceeding 90% and open-circuit voltage V_{oc} of 490 mV at a short current density J_{sc} of ~3A/cm^2 were reported [15,17]. Fill factors for GaSb cells are typically in the range 70-72%.

TPV cells generally operate at temperatures greater than 300 K, and the sensitivity of cell performance to temperature was studied. The temperature coefficients are slightly influence by the illumination level and the temperature dependence of V_{oc} was reported to be about -1.6 to –1.7 mV/K for incident power density between 1 and 6 W/cm^2, while FF was about –0.001/K [16]. A slightly lower value for the temperature coefficient of V_{oc} was also reported at –1.42 mV/K between 25 and 75°C [17].

2.2 Polycrystalline GaSb Cells

Production of GaSb cells can further be simplified and the process made more economical by using polycrystalline GaSb wafers [15,23]. Cells were fabricated using Zn diffusion, and cell

performance was only moderately lower by 8.7% for polycrystalline cells compared to single crystal ones [23]. It should be noted, however, that the change in performance will likely be sensitive to the average grain size, which was not reported. Nevertheless, these promising results have led to other efforts to grow bulk ternary crystals such as InGaSb for fabrication of lower-E_g cells [16,18].

2.3 Epitaxially Grown GaSb Cells

Although epitaxially grown GaSb cells will increase cost, the use of epitaxy can yield higher quality material as well as provide additional flexibility in device layer design. For example, a highly doped n-GaSb layer can be grown as a back surface field; AlGaAsSb can be grown as a window layer; and independent variation of base and emitter thickness and doping levels can be systematically studied. Both liquid phase epitaxy (LPE) and organometallic vapor phase epitaxy (OMVPE) have been used to prepare GaSb TPV cells [5,15,21]. In a comparison of cells fabricated from bulk GaSb vs LPE-grown material, it was reported that the internal QE increased from 90-92% to 96-97%, respectively [21]. Using OMVPE, GaSb cells were grown with and without an AlGaAsSb window layer [15]. The external QE of uncoated cells increased from less than 30% without the AlGaAsSb to over 60% with the AlGaAsSb. It was estimated that the surface recombination velocity S decreased from 10^6 cm/s without the layer to about 10^4 cm/s with the layer.

3. InPAsSb TPV CELLS

The InPAsSb quaternary alloy lattice matched to InAs can provide cells with E_g in the range 0.35 to 0.5 eV. However, the advantages of such low temperature TPV systems are not presently clear, and so there has been less research on these materials and InPAsSb TPV cell performance

has not been optimized [5,16,24-27]. InPAsSb has been grown by both OMVPE and LPE, but only LPE has been used for TPV cells. InPAsSb was grown lattice matched to InAs substrates, and cells have been fabricated by Zn diffusion into n-InPAsSb epilayers [5,16,25,27] as well as from epitaxially grown p-n structures [26]. Another variation was an epitaxially grown p-InPAsSb/n-InAs heterojunction cell [24]. The longest spectral response of a InPAsSb TPV cell is out to 4.3 μm, and maximum response was observed at 3 μm (shown in Fig. 2) [24]. An InPAsSb cell with E_g=0.45 eV and spectral response out to 2.8 μm had V_{oc} = 0.15 V at J_{sc} = 3 A/cm^2 [25]. The relatively low V_{oc} value may be due to a non-optimized layer structure, high surface recombination velocity from lack of surface passivation, as well as Auger recombination, which will be a dominate recombination mechanism in low-Eg materials. This materials system is at an early stage, and studies addressing the above issues are necessary to assess the potential of these materials for TPV cells.

4. GaInAsSb TPV CELLS

As discussed in the introduction, a wide range of E_g from 0.3 to 0.7 eV is accessible with lattice-matched GaInAsSb alloys, thus potentially making this material system the most versatile one in terms of matching TPV cell E_g to radiator temperature. Furthermore, higher-E_g AlGaAsSb alloys can effectively be incorporated in the device structure as surface passivation/window or back-surface-field layers [28-31]. While these quaternary alloys can be grown lattice-matched to either GaSb or InAs substrates, higher thermodynamic stability of the alloy is achieved for epilayers lattice-matched to GaSb [32]. Therefore, these GaInAsSb cells have utilized epitaxial layers grown on GaSb.

High-performance GaInAsSb TPV cells have been prepared by all the major epitaxial technologies, including LPE [5,16,26,27,30,33,34], molecular beam epitaxy (MBE) [28,29,35,36], and OMVPE [28,29,37-42]. The IQE of LPE-grown cells is approaching 90%, while MBE- and OMVPE-grown cells exceed 95%. The spectral response of these cells shows various cut-off wavelengths due to the different GaInAsSb alloy composition that was used. Similarly, reported values of V_{oc} can vary as a result of the different E_g of the GaInAsSb alloy. Therefore, meaningful comparisons of V_{oc} data that are reported in the literature require a standardization methodology. In a best effort to compare these results, this paper will state voltage factors, defined as V_{oc} normalized to qE_g, where q is electronic charge. V_{oc} is taken at J_{sc} ~ 3 A/cm^2 whenever possible. The change in V_{oc} with J_{sc} at high illumination intensity is reported to be similar for cells independent of epitaxial preparation and is ~ 15 mV/A [28,34,36,39]. This dependence will be indicated when used to compare cells. The value used for E_g is estimated from the point of 50% decrease in QE from the spectral response curve. An additional point of reference for E_g is the 300 K photoluminescence (PL) peak energy minus 0.0125 eV due to the thermal distribution of electrons at the bandedge.

4.1 LPE-Grown GaInAsSb TPV Cells

The more cost-effective LPE process has been used to produce both epitaxially grown and Zn-diffused p-n structures [5,16,26,30,33,34]. The Zn-diffusion process was performed in a similar manner as discussed for GaSb cells, and Zn profiles were controlled to optimize carrier collection [33,34]. At J_{sc} = 3A/cm^2, V_{oc} is 344 mV for a ~0.6-eV cell, which results in qV_{oc}/E_g ~ 0.58. The maximum IQE is slightly less than 90% and the spectral response drops to about zero at ~2.2 μm. Another study of LPE grown p-n GaInAsSb structures reported a maximum IQE of about 85% for cells with a slightly longer spectral response out to ~2.3 μm [30]. The

temperature coefficients of GaInAsSb cells are slightly smaller than those measured for GaSb cells, and the temperature dependence of V_{oc} was reported to be -1.5 mV/K at an incident power density of 3 W/cm^2, while FF was about –0.001/K.

4.2 OMVPE- and MBE-Grown GaInAsSb TPV Cells

Extending the spectral response of GaInAsSb TPV cells beyond 2.3 μm has been of interest for TPV systems operating at low radiator temperatures. In principle, the E_g of the lattice-matched GaInAsSb/GaSb alloy can be as low as 0.3 eV. However, equilibrium thermodynamics predicts a large miscibility gap, which results in a tendency for the alloy to phase separate into regions of non-uniform composition [32]. Thus, in practice, this makes it difficult to grow high quality alloys with $0.3 < E_g < 0.55$ under conditions of near thermodynamic equilibrium. Alloy phase separation deleteriously impacts structural and optical properties of the alloy, which in turn causes the minority-carrier lifetime to be degraded by defect-mediated recombination mechanisms. Ultimately, TPV device performance will be limited.

Therefore, concerted efforts have been made to grow high-quality materials in which minority-carrier recombination is radiatively limited. OMPVE has been used to develop these GaInAsSb materials, and growth kinetics has been shown to be very effective in suppressing phase separation [43]. While MBE can also be used and has already been extensively developed for laser diodes [44], the higher growth rates attainable in OMVPE as well as the use of miscut substrates, which will be discussed further, make OMVPE more attractive for growth of TPV structures, which are typically ~5-6 μm thick. Furthermore, a high level of control over alloy composition, doping level, layer thickness, and interface growth has been achieved not only in single wafer reactors [41], but also multi-wafer reactors [40]. Since the few reports of MBE-

grown TPV cells use similar device architectures as those grown by OMVPE, for completeness, results of those cells are briefly referenced in this section.

4.2.1 GaInAsSb OMVPE Materials

High-quality GaInAsSb materials that are radiatively limited increase enhancements that might be obtained by photon recycling, as will be discussed in a later section. Alloys with E_g as low as 0.5 eV were optimized by correlating OMVPE growth conditions with extensive materials characterization. Details of these studies were previously reported [37-39,43,45], and the main points are briefly summarized. It was shown that phase separation in epitaxial growth is a surface-mediated process and material quality could be greatly improved by reducing adatom surface diffusivity. This was achieved by decreasing growth temperature; increasing adatom flux (i.e., growth rate); and increasing substrate miscut angle.

Figure 3 shows representative results of high-quality 0.50-eV GaInAsSb that was grown at 525 °C. The atomic force microscopy scan of the surface, shown in Fig. 3a, indicates a very smooth vicinal surface and implies ideal step-flow growth. Figure 3b shows the high-resolution x-ray diffraction curve, which is a measure of the lattice constant of the material. The full-width at half-maximum (FWHM) value of the peak associated with the epilayer is comparable to that of the substrate, and is indicative of high structural quality and compositional uniformity. Alloy uniformity is further confirmed by the observation of uniform contrast in the cross-sectional transmission electron microscopy image shown in Fig. 3c. Finally, high optical quality is evident in 4- and 300-K photoluminescence (PL) spectra, shown in Fig. 3d. The 4-K FWHM PL peak is only 9.5 meV, and the wavelength shift between 4- and 300-K PL peaks corresponds to the expected E_g dependence on temperature of ~0.07 eV.

4.2.2 GaInAsSb TPV Cell Studies

The device architecture that has been developed for high-performance GaInAsSb TPV cells, grown either by OMVPE or MBE, is shown in Figure 4. It consists of a thicker p-GaInAsSb emitter layer compared to the n-GaInAsSb base layer in order to take advantage of the longer minority carrier diffusion lengths in the p-layer [29,31,46]. The use of a higher-E_g window layer is critical for reducing losses due to surface recombination, and both GaSb and AlGaAsSb windows are effective surface passivation layers [28-31,35,38-41]. Specific details of TPV cell performance are described in this section.

The doping level of the p-type emitter layer plays a stronger role in TPV cell performance than that in the n-type base layer, since the emitter layer is about 4 to 5 times thicker. To study the effect of emitter doping level on TPV cells, the doping level of the 3-5-μm-thick emitter layer was varied in the range between 10^{17} $cm^{-3}$and 10^{18} cm^{3} while doping in the 0.2-1-μm-base layer doping was ~5 x 10^{17} cm^{-3}. Figure 5 shows the EQE of uncoated 0.53-eV GaInAsSb/AlGaAsSb TPV cells, and Table 1 summarizes V_{oc}, FF, series resistance R_s and dark current I_s. The data are averaged from 4 to 6 cells per structure. A high EQE of 66-67% is observed for cells with doping level of 1 to 2 x 10^{17} cm^{-3}. The EQE is slightly lower at 64% with a higher doping level of 4 x 10^{17} cm^{-3}, and is still lower at 62% with doping of 10 x 10^{17} cm^{-3}. Even this lowest value of EQE corresponds to an IQE of 92%.

Table 1 shows that series resistance R_s decreases with increasing doping, as expected. On the other hand, at J_{sc} of 3 A/cm^2, V_{oc} is 316 mV for the lowest doped sample and is slightly higher at 321 mV for the highest doping level. The voltage factor for all these devices is qV_{oc}/E_g is 0.6. The FF increases from 68 to almost 71% with increasing doping, and can be most likely explained by the decreasing R_s values at higher doping levels. A drift-diffusion model [47] was used with inputs that were parametrically varied to qualitatively study this cell performance data.

The relatively small sensitivity of cell performance to doping in the emitter is indicative of the high quality of the GaInAsSb bulk layers and interfacial growth, and consistent with long minority carrier diffusion lengths L, which are estimated to be greater than 10 μm even for the highest doped sample, and low surface recombination velocity S, which has been reported to be below 1000 cm/s [48-50].

The EQE, reflectivity, and IQE of a cell with similar structure and low emitter doping level are shown in Fig. 6, and V_{oc} vs J_{sc} is shown in Fig. 7. The IQE exceeds 95% between 1.4 and 2.05 μm, and qV_{oc}/E_g is 0.6. TPV cells with different GaInAsSb alloy composition were tested to determine the effect of E_g on cell performance. Figure 8 shows the IQE for three different TPV cells with E_g of 0.58, 0.53, and 0.49 eV, with spectral response out to 2.25, 2.5 and 2.7 μm, respectively. The IQE exceeds 95% for all cells, and the longest spectral response is observed out to 2.7 μm.

$qVoc/E_g$ data for homojunction GaInAsSb TPV cells are plotted as a function of E_g in Fig. 9. Data are included for cells for cells grown with either GaSb or AlGaAsSb window layers, and have been nominally corrected for V_{oc} at J_{sc} of 3 A/cm^2. Data for our OMVPE-grown cells typically represent an average of three to six cells, and the standard deviation of qV_{oc}/E_g does not exceed 0.015. Also shown are the published data for diffused-junction GaInAsSb cells [16,33,34], the best-reported GaSb cells [17], InPAsSb cells [25], and the practical qV_{oc}/E_g limit at J_{sc} at 3 A/cm^2 [51]. GaSb cells have a voltage factor that is within 90% of this limit. The voltage factor for GaInAsSb cells depends on E_g. It is 87% of the limit for 0.58-eV GaInAsSb cells, but decreases to 76% for 0.49-eV GaInAsSb cells. It further decreases to 54% of the limit for 0.45-eV InPAsSb cells. The degradation in voltage factor with decreasing E_g may be due to Auger recombination, which becomes more dominant, as well as to non-optimized cell

structures. Materials studies to characterize Auger coefficients of these lower E_g materials would be useful for further interpretation of device results.

4.2.3 Current Work on Further Enhancements in GaInAsSb TPV Cells

As discussed above, GaInAsSb/AlGaAsSb/GaSb TPV cells exhibit peak internal quantum efficiency and fill factor values that are approaching theoretical limits. On the other hand, qV_{oc}/E_g values are between 13 to 24 % below the theoretical limit, and depend on E_g of the TPV cell. Therefore, emphasis of current work is to understand factors that may be limiting cell performance in order to better understand how to increase the voltage factor. Modeling TPV cell performance [35,52] is gradually become more meaningful as fundamental materials properties and recombination parameters are experimentally established [49,50,53]. Recent studies of minority-carrier lifetime of OMPVE-grown GaInAsSb lifetime structures suggest that the material is radiatively limited [53]. Therefore, photon recycling effects could play an important role in enhancing GaInAsSb TPV cell performance [54]. This can be implemented by incorporating a back-surface reflector (BSR). Another approach to increase V_{oc} is to use tandem cells. GaSb and GaInAsSb cells with an internal connecting tunnel junction were fabricated by LPE and V_{oc} of 0.6 eV was reported [5]. A third approach is to use AlGaAsSb/GaInAsSb heterojunctions that are designed to decrease dark current [36]. A 5% increase in V_{oc} was reported for the heterojunction compared to the homojunction [36].

Our approach has been to incorporate a BSR, and our initial studies of GaInAsSb cells with a BSR showed a fractional increase in EQE of about 20% near the band-edge [41], and only a nominal increase of 4 mV in V_{oc} [55]. Modeling studies predict that the voltage increase due to photon recycling is extremely sensitive to surface recombination velocity S, and should be lower than 100 cm/s to take full advantage of this effect [56]. Therefore, since bulk lifetimes t_{BLK} are

high, the present TPV cells could be limited by S, even though S has been reported to be less than 500 cm/s [35,41,49,50]. This can be explained by the fact that V_{oc} is more sensitive to surface recombination velocity than J_{sc} because under short-circuit conditions, photo-generated carriers quickly diffuse out of the emitter, while under open-circuit conditions, the long bulk recombination time increases the probability that these photo-generated electrons will diffuse to the emitter/window interface and recombine. Further device studies coupled with device modeling would provide further insight for guiding efforts to improve the voltage factor.

To minimize recombination at the GaInAsSb/AlGaAsSb heterointerface, we recently modified OMVPE growth processes to reduce S [57,58]. The inverse electron lifetime, $1/\tau_{PL}$, of AlGaAsSb/GaInAsSb/AlGaAsSb DHs with the p-type active layer doped at 2 x 10^{17} cm^{-3} is shown in Fig. 10 as a function of inverse active layer thickness, 1/W. Data for two sets of samples with different Al content of 0.2 and 0.25 demonstrate a linear dependence, and S is determined as previously described [49] to be 46 and 27 cm/s for Al content in AlGaAsSb of 0.2 and 0.25, respectively. The difference in these values is probably not significant. These low values are significantly smaller than the value of 720 cm/s that was previously reported [49], which is reduced to ~500 cm/s after taking photon recycling into account.

Also shown in Fig. 10 for comparison is t_{PL} for a DH sample with p-GaSb capping layers. Assuming that GaSb capped DHs would have the same t_{BLK} value (53 ns) as AlGaAsSb capped samples, an estimate of S with GaSb capping layers yields a significantly higher value of S ~250 cm/s. Therefore, from both band-structure considerations and experimental results [49], there appears to be an advantage of AlGaAsSb over GaSb as the window layer. The valence-band offset between ~0.53-eV $Ga_{0.84}In_{0.16}As_{0.14}Sb_{0.86}$ and $Al_{0.25}Ga_{0.75}As_{0.02}Sb_{0.98}$ is almost zero, while the GaInAsSb/GaSb interface is a staggered type-II band alignment. The former alignment

minimizes carrier trapping at the heterointerface, and consequently, these heterostructures should have a comparatively lower surface recombination velocity, as has been consistently observed.

This reduction in S is expected to make a more significant difference in improving V_{oc} in TPV cells that are grown under these new optimized OMVPE conditions.

4.2.4 Monolithic Series Interconnection of GaInAsSb TPV Cells

Monolithic series interconnection of InGaAs/InP TPV cells has been developed to build V_{oc}; reduce parasitic losses; and simplify module assembly [59-61]. InGaAs Monolithically interconnected modules (MIMs) were fabricated on semi-insulating (SI) InP substrates, which is relatively straightforward compared to GaInAsSb MIMs since SI GaSb substrates are unavailable. In order to assess the feasibility of on-wafer device isolation of GaInAsSb cells, two different approaches for were studied. One approach is the use of a lattice-matched AlGaAsSb cell-isolation diode as a buffer layer below the GaInAsSb/GaSb TPV cell. Modest voltage building was achieved for 0.6-eV TPV cells and V_{oc} of 0.42 V for a 15-cell MIM was reported [62]. A second approach that we have pursued is to wafer bond the GaSb-based epilayers to a SI GaAs handle wafer, remove the GaSb substrate, and then process the wafer-bonded (WB) epitaxy [63-65]. Although the fabrication is more involved, wafer bonding is a common practice not only in Si microelectronics but also in the fabrication of high-performance light emitting diodes.

Figure 11 schematically illustrates the WB device. The bonding layer is a composite structure of SiO_x/Ti/Au. Au is used as the material to bond the GaSb to GaAs, while the SiO_x dielectric layer provides both electrical isolation and enhanced reflectivity in combination with Au. Ti is used to improve the adhesion of Au to SiO_2. This high reflectivity layer was shown to be very effective as an internal BSR to increase take advantage of photon recycling [65]. WB

lifetime test structures have PL intensity about 4 times higher for the WB sample compared to the unbonded control samples. Furthermore, t_{PL} is more than two times higher at 85 ns for the WB sample compared to the control sample with t_{PL} = 36 ns. These results show that photons that might normally be absorbed in a doped GaSb substrate are reflected back to the active layer and reabsorbed. Thus, the internal BSR is effective in increasing minority-carrier lifetime through photon recycling.

The peak EQE of uncoated WB TPV devices is 62%, which is comparable to that of conventional TPV cells. The goal to build V_{oc} was achieved and results are shown in Fig. 12 for a single-junction TPV cell and 2- and 10-junction series-interconnected TPV cells. At J_{sc} ~ 0.4 A/cm^2, the single cell exhibits V_{oc} ~ 0.2 V. At this same current density, V_{oc} is 0.37 and 1.8 V for the 2- and 10-junction devices, respectively. These results indicate that nearly linear voltage building has been achieved. At higher J_{sc} ~ 1 A/cm^2, V_{oc} is ~ 0.470 and 2.0 V for the 2- and 10-junction devices, respectively. The fill factor FF of the 2-junction device is about 51% at J_{sc} ~ 0.4 A/cm^2, and degrades to about 38% at J_{sc} ~ 1 A/cm^2. This degradation is related to high series resistance in the cell-to-cell interconnections, and could be reduced with improved metallization and reduced resistance in the n-GaSb lateral conduction layer. Further reduction in series resistance could probably be achieved by contacting the n-GaInAsSb, which can have lower contact resistivity and sheet resistance than n-GaSb [66].

CONCLUSIONS

This paper briefly reviewed the current status of antimony-based III-V thermophotovoltaic (TPV) cells, which have a large range of E_g, and therefore have been of particular interest for TPV generators operating with low radiator temperatures. The spectral response can be tuned out to 1.7 µm for GaSb cells, 2.7 µm for GaInAsSb cells, and 4.3 µm for InPAsSb cells. While

quantum efficiency and fill factor have been more easily optimized to approach theoretical limits, open-circuit voltage factors near that limit have been more difficult to achieve. The voltage factor is highest at 90% of the limit for GaSb cells, and decreases with decreasing E_g for the quaternary alloys. It is over 85% of the limit for 0.53-eV GaInAsSb cells, but decreases below 80% for 0.49-eV GaInAsSb cells, and is only 54% for InPAsSb cells. A reasonable explanation may be related to the relatively immature status of cells with $E_g < 0.5$ eV, which have not received the same extent of research focus as the higher E_g materials. However, it is also likely that this lower performance is due to Auger recombination, which can be the dominant minority-carrier recombination mechanism in low E_g materials. Fundamental materials measurements of radiative and Auger recombination coefficients combined with device modeling are necessary to provide further insights for future device improvements of lower E_g TPV cells. In the nearer term, structural changes in device architecture of GaInAsSb cells, such as the incorporation of back-surface reflectors, monolithic tandem cells, and heterojunctions are being evaluated to enhance voltage factors.

ACKNOWLEDGMENTS

The author gratefully acknowledges invaluable contributions of numerous colleagues during the course of our GaInAsSb TPV research, and is especially indebted to collaborations with H.K. Choi, C.J. Vineis, R.K. Huang, M.K. Connors, D. Calawa, G.W. Charache, L.R. Danielson, G. Nichols, M. Dashiell, D. Donetsky, S. Anikeev, G. Belenky, J.M. Borrego, and I. Bhat. This work was sponsored by the Department of Energy under AF Contract No. F19628-00-C-0002. The opinions, interpretations, conclusions and recommendations are those of the author and are not necessarily endorsed by the United States Government.

REFERENCES

1. 5th Conference on Thermophotovoltaic Generation of Electricity, eds. T.J. Coutts, G. Guazzoni, and J. Luther, AIP Conf. Proc. 653 (2003) Melville, NY.
2. T.J. Coutts, "A review of progress in thermophotovoltaic generation of electricity," Renewable and Sustainable Energy Reviews **3**, 77-184 (1999).
3. P.F. Baldasaro, J.E. Raynolds, G.W. Charache, D.M. DePoy, C.T. Balllinger, T. Dovovan, and J.M. Borrego, "Thermodynamic analysis of thermophotovoltaic efficiency and power density tradeoffs," J. Appl. Phys. **89**, 3319-3327 (2001).
4. B. Bitnar, J.-C. Mayor, W.Durisch, A. Meyer, G. Palfinger, F. von Roth, and H. Sigg, "Record Electricity-to-Gas Power Efficiency of a Silicon Solar Cell Based TPV System, AIP Conf. Proc. 543, pp. 18-28 (2003).
5. V.M. Andreev, "An Overview of TPV Cell Techonologies," AIP Conf. Proc. 653, pp. 289-304 (2003).
6. L.M. Frass, "TPV Tube Genertors for Apartment Building and Industrial Furnace Applications," AIP Conf. Proc. 653, pp. 38-48 (2003).
7. B. Wernsmann, R.R. Siergiej, S.D. Link, R.G. Mahorter, M.N. Palmisiano, R.J. Wehrer, R.W. Schultz, G.P. Schmuck, R.L. Messham, S. Murray, C.S. Murray, F. Newman, D. Taylor, D.M. DePoy, and T. Rahmlow, "Greater than 20% Radiant Heat Conversion Efficiency of a Thermophotovoltaic Radiator/Module System using Reflective Spectral Control," IEEE Trans. Electron. Dev. **51**, 512-515 (2004).

8. J. Beausang, "Thermodynamic Analysis of Thermophotovoltaic Efficiency and Power Density Tradeoffs," presented at 5th Conference on Thermophotovoltaic Generation of Electricity, Rome, Italy, 16-19 Sept. 2002.
9. Y.Z. Yu, R.U. Martinelli, G.C. Taylor, Z. Shellenbarger, R.K. Smeltzer, J. Li, K. Palit, S.R. Burger, R.P. Cardines, L.R. Danielson, C.A. Wang, and M.K. Connors, "High-Efficiency Multi-Cell TPV Module Fabrication and Performance," AIP Conf. Proc. 653, pp. 335-343 (2003).
10. G.W. Charache, P.F. Baldasaro, L.R. Danielson, D.M. DePoy, M.J. Freeman, C.A. Wang, H.K. Choi, D.Z. Garbuzov, R.U. Martinelli, V. Khalfin, S. Saroop, J.M. Borrego, and R.J. Gutman, "InGaAsSb thermophotovoltaic diode: Physics evaluation," J. Appl. Phys. **85**, 2247-2252 (1999).
11. Y.Z. Liu, H.T. Yang, and J.S. Harris, Jr., "Low Bandgap (0.7 to 1.1 eV) Solar Cells in the GaAlAsSb/GaSb System," Proc. 14th IEEE Photovoltaics Spec. Conf., pp. 341-345 (1980).
12. L.M. Fraas, G.R. Girard, J.E. Avery, B.A. Arau, V.S. Sundaram, A.G. Thompson, and J.M. Gee, "GaSb booster cells for over 30% efficient solar-cell stack," J. Appl. Phys. **66**, 3866-3870 (1989).
13. A.C. Day, W.E. Horne, and M.D. Morgan, "Application of the GaSb Solar Cell in Isotope-Heated Power Systems," Proc. 21st IEEE Photovoltaics Spec. Conf., pp. 1320-1325 (1990).
14. L. Fraas, R. Ballantyne, J. Samaras, and M.Seal, "Electric Power Production Using New GaSb Photovoltaic Cells with Extended Infrared Response," AIP Conf. Proc. 321, pp. 44-53 (1995).

15. A.W. Bett and O.V. Sulima, “GaSb photovoltaic cells for applications in TPV generators,” Semi. Sci. Tech. **18**, S184-S190 (2003).

16. O.V. Sulima, A.W. Bett, M.G. Mauk, F. Dimroth, P.S. Dutta, and R.L. Mueller, “GaSb-, InGaAsSb-, InGaSb-, InAsSbP, and Ge-TPV cells for low temperature TPV applications,” AIP Conf. Proc. 653, pp. 434-441 (2003).

17. O.V. Sulima and A.W. Bett, “Fabrication and simulation of GaSb thermophotovoltaic cells,” Solar Energy Mat. And Solar Cells **66**, 533-540 (2001).

18. P.S. Dutta, J.M. Borrego, H. Ehsani, G. Rajagopalan, I.B. Bhat, R.J. Gutman, G. Nichols, and P.F. Baldasaro, “GaSb and $Ga_{1-x}In_xSb$ Thermophotovoltaic Cells using Diffused Junction Technology in Bulk Substrates,” AIP Conf. Proc. 653, pp. 392-401 (2003).

19. L.B. Karlina, B. Ya.Ber, P.A. Blagnov, M.M. Kulagina, and A.s. Vlasov, “Zinc(P) diffusion in $In_{0.53}Ga_{0.47}As$ and GaSb for TPV devices,” AIP Conf. Proc. 653, pp. 373-382 (2003).

20. C. Algora and D. Martin, “Modelling and Manufacturing GaSb TPV Converters,” AIP Conf. Proc. 653, pp. 452-461 (2003).

21. V.M. Andreev, V.P. Khvostikov, V.D. Rumyantsev, S.V. Sorokina, M.Z. Shvarts, “Single-Junction GaSb and Tandem GaSb/InGaAsSb/ and AlGaAsSb/GaSb Thermphotovoltaic Cells,” Conf. Record of 28th IEEE Photovoltaic Spec. Conf., pp. 1265-1268 (2000).

22. Fourth NREL Thermophotovoltaic Generation of Electricity, eds. T.J. Coutts, J.P. Benner, and C.S. Allman, AIP Conf. Proc. 460, (1999) New York.

23. L. Frass, R. Ballantyne, S. Hui, S-Z. Ye, S. Gregory, J. Keyes, J.A. Avery, D. Lamson, and B. Daniels, "Commercial GaSb Cell and Circuit Development for Midnight Sun TPV Stove, AIP Conf. Proc. 460, pp. 480-487 (1999).

24. V.A. Gevorkyan, V.M. Aroutiounian, K.M. Gambaryan, M.S. Kazaryan, K.J. Touryan, and M.W. Wanlass, "Liquid-phase electroepitaxial growth of low band-gap p-InAsPSb/n-InAs and p-InAsP/n-InAs diode heterostructures for thermo-photovoltaic application," Thin Solid Films **451-452**, 124-127 (2004).

25. V.M. Andreev, V.P. Khvostikov, O.V. Khvostikova, E.V. Oliva, V.D. Rumyantseva, M.Z. Shvarts, and T.S. Tabrarov, "Low-bandgap Ge and InAsSbP/InAs-based TPV Cells," AIP Conf. Proc. 653, pp. 383-391 (2003).

26. M.G. Mauk, M.G., Z.A. Shellenbarger, J.A. Cox, J.A., O.V. Sulima, A.W. Bett, R.L. Mueller, P.E. Sims, J.B. McNeely, L.C. DiNetta, "Liquid-phase epitaxy of low-bandgap III-V antimonides for thermophotovoltaic devices," Journal of Crystal Growth **211**, 189-193 (2000).

27. M.G. Mauk and V.M. Andreev, "GaSb-related materials for TPV cells," Semicond. Sci. Technol. **18**, S191-S201 (2003).

28. H. Choi, C.A. Wang, G.W. Turner, M.J. Manfra, D.L. Spears, G.W. Charache, L.R. Danielson, and D.M. Depoy, "High-Performance GaInAsSb Thermophotovoltaic Devices with an AlGaAsSb Window," Appl. Phys. Let. **71**, 3758-3760 (1997).

29. C.A. Wang, H.K. Choi, G.W. Turner, D.L. Spears, and M.J. Manfra, "Lattice-matched epitaxial GaInAsSb/GaSb thermophotovoltaic devices," AIP Conference Proceedings 401, pp. 75-87 (1997) .

30. Z.A. Shellenbarger, M.G. Mauk, J.A. Cox, M.I. Gottfried, P.E. Sims, J.D. Lesko, J.B. McNeely, L.C. DiNetta, and R.L. Mueller, "Improvements in GaSb-Based Thermophotovoltaic Cells" AIP Conf. Proceedings 401, pp. 117-128 (1997).
31. C.W. Hitchcock, R.J. Gutman, J.M. Borrego, I.B. Bhat, and G.W. Charache, "Antimonide-Based Devices for Thermophotovoltaic Applications," IEEE Trans. Electron. Dev. 46, 2154-2161 (1999).
32. M.J. Cherng, H.R. Jen, C.A. Larsen, G.B. Stringfellow, H. Lundt, and P.C. Taylor, "MOVPE Growth of GaInAsSb," J. Cryst. Growth **77**, 408-417 (1986).
33. A.W. Bett, B.Y. Ber, M.G. Mauk, J.T. South, and O.V. Sulima, "Pseudo-Closed Box Diffusion of Zn into InGaAsSb and AlGaSb for TPV Devices," AIP Conf. Proceedings 460, pp. 237-246(1998) .
34. O.V. Sulima, R. Beckert, A.W. Bett, J.A. Cox, and M.G. Mauk, "InGaAsSb Photovoltaic Cells with Enhanced Open-Circuit Voltage" IEE Proc.-Optoelectronics **147**, 199-204 (2000).
35. V.B. Khalfin, D.Z Garbuzov, H. Lee, G.C. Taylor, N. Morris, R.U. Martinelli, and J.C. Connolly, "Interfacial Recombination in In(Al)GaAsSb/GaSb Thermophotovoltaic Devices," AIP Conf. Proceedings 460, pp. 247-255 (1998).
36. D.Z. Garbuzov, R.U. Martinelli, V. Khalfin, H. Lee, N.A. Morris, G.C. Taylor, J.C. Connolly, G.W. Charache, and D.M. DePoy, "A Novel Approach for the Improvement of Open-Circuit Voltage and Fill Factor of InGaAsSb/GaSb Thermophotovoltaic Cells,"AIP Conf. Proc. 420, pp. 1400-1409 (1998).

37. C.A. Wang, H.K. Choi, D.C. Oakley, and G.W. Charache, “Recent progress in GaInAsSb thermophotovoltaics grown by organometallic vapor phase epitaxy,” J. Cryst. Growth **195**, 346-355 (1998).

38. C.A. Wang, H.K.Choi, S.L. Ransom, G.W. Charache, L.R. Danielson, and D.M. DePoy, “High-quantum-efficiency 0.5 eV GaInAsSb/GaSb thermophotovoltaic devices,” Appl. Phys. Lett. **75**, 1305-1307 (1999).

39. C.A. Wang, H.K. Choi, G.W. Charache, “Epitaxial Growth of GaInAsSb for Thermophotovoltaic Devices,” IEE Proc. Optoelectron. **147**, 193-198 (2000).

40. Z.A. Shellenbarger, G.C. Taylor, R.K. Smeltzer, J. Li, R.U. Martinelli, and K. Palit, “High Performance InGaAsSb TPV Cells via Multiwafer OMVPE Growth,” AIP Conf. Proc. 653, pp. 314-323 (2003).

41. C.A. Wang, C.J. Vineis, H.K. Choi, M.K. Connors, R.K. Huang, L.R. Danielson, G. Nichols, G.W. Charache, D. Donetsky, S. Anikeev, and G. Belenky, “Lattice-Matched GaInAsSb/AlGaAsSb/GaSb Materials for Thermophotovoltaic Devices,” AIP Conf. Proc. 653, pp. 324-334 (2003).

42. J.G. Cederberg, M.J. Hafich, R.M. Biefeld, and M. Palmissiano, “The preparation of InGa(As)Sb and Al(Ga)AsSb films and diodes on GaSb for thermophotovoltaic applications using metal-organic chemical vapor deposition,” J. Cryst. Growth **248**, 289-295 (2003).

43. C.A. Wang, “Correlation between surface step structure and phase separation in epitaxial GaInAsSb,” Appl. Phys. Lett. **76**, 2077 (2000).

44. A. Joullie, P. Christol, A.N. Baranov, and A. Vicet, "Mid-infrared 2-5 μm heterojunction laser diodes," in Solid Sate Mid-Infrared Laser Sources, eds. I.T. Sorokina, K.L. Vodopyanov, Springer (New York, 2003) pp 1-59.

45. C.A. Wang, "Progress and Continuing Challenges in GaSb-Based III-V Alloys and Heterostructures Grown by Organometallic Vapor Phase Epitaxy," 12th Intl. Conf. on Metalorganic Vapor Phase Epitaxy, Lahaina, Hawaii, 2004, and J. Cryst. Growth.

46. R.U. Martinelli, D.Z. Garbuzov, H. Lee, N. Morris, T. Odubanjo, G.C. Taylor, and J.C. Connolly, "Minority-Carrier Transport in InGaAsSb Thermophotovoltaic Diodes," AIP Conf. Proc. 401, pp. 389-395 (1997).

47. H.J. Moeller, Semiconductors for Solar Cells, Artech House, Boston, 1993.

48. S. Saroop, J.M. Borrego, R.J. Gutman, G.W. Charache, C.A. Wang, "Recombination processes in doubly capped antimonide-based quaternary alloys," J. Appl. Phys. **86**, 1527-1534 (1999).

49. D. Donetsky, S. Anikeev, G. Belenky, S. Luryi, C. A. Wang, and G. Nichols, "Reduction of interfacial recombination in GaInAsSb/AlGaAsSb/GaSb double heterostructures," Appl. Phys. Lett., **81**, 4769-4771 (2002).

50. R.J. Kumar, R.J. Gutmann, J.M. Borrego, P.S. Dutta, C.A. Wang, R.U. Martinelli, G. Nichols, " Recombination Parameters for Antimonide-Based Semiconductors Using the Radio Frequency Photoreflectance Technique," J. Electron. Mater. **33**, 94-100 (2003).

51. P.F. Baldasaro, E.J. Brown, D.M. DePoy, B.C. Campbell, and J.R. Parrington, "Experimental Assessment of Low Temperature Voltaic Energy Conversion," AIP Conf. Proc. 321, pp. 29-43 (1995).

52. J.M Borrego, C.A. Wang, P.S. Dutta, G. Rajagopalan, R.J. Gutman, I.B. Bhat, H. Ehsani, J.F. Beausang, G. Nichols, and P.F. Baldasaro, “Performance Limits of Low Bandgap Thermophotovoltaic Antimonide-Based Cells for Low Temperature Radiators,” AIP Conf. Proc. 653, pp. 498-507 (2003).
53. S. Anikeev, D. Donetsky, G. Belenky, S. Luryi, C. A. Wang, J.M. Borrego, and G. Nichols, “Measurement of the Auger recombination rate in p-type 0.54-eV GaInAsSb by time-resolved photoluminescence,” Appl. Phys. Lett., **83**, 3317-3319 (2003).
54. J.M. Borrego, S. Saroop, R.J. Gutman, G.W. Charache, T. Donovan, P.F. Baldasaro, C.A. Wang, “J. Appl. Phys. **89**, 3753 (2001).
55. R.K. Huang, C.A. Wang, M.K. Connors, G.W. Turner, M. Dashiell, “Hybrid Back-Surface Reflector GaInAsSb Thermophotovoltaic Devices,” to be presented 6th Conference on Thermophotovoltaic Generation of Electricity, 14-16 June 2004 Freiburg, Germany.
56. M. Dashiell et al, to be presented 6th Conference on Thermophotovoltaic Generation of Electricity, 14-16 June 2004, Freiburg, Germany.
57. C.A. Wang, D.A. Shiau, D. Donetsky, S. Anikeev, G. Belenky, S. Luryi, “Effect of Growth Interruption on Surface Recombination Velocity in GaInAsSb/AlGaAsSb Heterostructures Grown by Organometallic Vapor Phase Epitaxy,” to be presented 12th International Conference on Metal Organic Vapor Phase Epitaxy, 30 May-4 June 2004, Lahaina, Hawaii,.
58. D. Donetsky et al, to be presented 6th Conference on Thermophotovoltaic Generation of Electricity, 14-16 June 2004 Freiburg, Germany.

59. N.S. Fatemi, D. M. Wilt, R.W. Hoffman, Jr., M.A. Stan, V.G. Weizer, P.P. Jenkins, O.S. Khan, C.S. Murray, D. Scheiman, D. Brinker, AIP Conf. Proc. 460, 121-131 (1999).

60. M.W. Wanlass, J.J. Carapella, A. Duda, K. Emery, L. Gedvilas, T. Moriaty, S. Ward, and J.D. Webb, X. Wu, AIP Conf. Proc 460, 132-141 (1999).

61. R.R. Siergiej, B. Wernsmann, S.A. Derry, R.G. Mahorter, R.J. Wehrer, S.D. Link, M.N. Palmisiano, R.L. Messham, S. Murray, C.S. Murray, F. Newman, J. Hills, and D. Taylor, "20% Efficient InGaAs/InPAs Thermophotovoltaic Cells," AIP Conf. Proc. 653, pp. 414-423 (2003).

62. N.M. Palmisiano, R.M. Biefeld, J.G. Cederberg, M.J. Hafich, and G.M. Peake, "Development of InGaAsSb Based Monolithic Interconnected Modules" to be published in The Fifth Conference on Thermophotovoltaic Generation of ElectricityM.N. Palmisiano, R.M. Biefeld, J.G. Cederberg, M.J. Hafich, and G.M. Peake, AIP Conf. Proc. 653, 305-313 (2003).

63. C.A. Wang, P.G. Murphy, P.W. O'Brien, D.A. Shiau, A.C. Anderson, Z.L. Liau, D.M. DePoy, and G. Nichols, "AIP Conf. Proc. 653, 473-481 (2003).

64. C.A. Wang, R.K. Huang, D.A. Shiau, M.K. Connors, P.G. Murphy, P.W. O'Brien, A.C. Anderson, D.M. DePoy, G. Nichols, and M.N. Palmisiano, "Monolithically series-interconnected GaInAsSb/AlGaAsSb/GaSb thermophotovoltaic devices with an internal backsurface reflector formed bonding," Appl. Phys. Lett. **83**, 1286-1288 (2003).

65. C.A. Wang, R.K. Huang, M.K. Connors, D.A. Shiau, P.G. Murphy, P.W. O'Brien, A.C. Anderson, D. Donetsky, S. Anikeev, G. Belenky and S. Luryi, G. Nichols, "Monolithically Series-Interconnected GaInAsSb/AlGaAsSb Thermophotovoltaic Devices

Wafer Bonded to GaAs," to be presented 6th Conference on Thermophotovoltaic Generation of Electricity, 14-16 June 2004 Freiburg, Germany.

66. C.A. Wang, D.A. Shiau, R.K.Huang, C.T. Harris, and M.K. Connors, "Organometallic vapor phase epitaxy of n-GaSb and n-GaInAsSb for low resistance ohmic contacts," J. Cryst. Growth **261**, 379-384 (2004).

LIST OF FIGURES

Figure 1. Bandgap vs. lattice constant of antimonide-based III-V alloys.

Figure 2. Spectral response of GaSb [17], GaInAsSb, and InPAsSb [24] TPV cells. Efficiency has been scaled for comparison.

Figure 3. Materials characterization results of 0.5-eV GaInAsSb grown by OMVPE: (a) atomic force microscopy image, (b) high-resolution x-ray diffraction, (c) cross-sectional transmission electron microscopy, and (d) 300- and 4-K photoluminescence.

Figure 4. Schematic structure of GaInAsSb/AlGaAsSb/GaSb TPV cells. The AlGaAsSb window layer is sometimes omitted from the structure.

Figure 5. Spectral response of 0.53-eV GaInAsSb/AlGaAsSb/GaSb TPV cells with various p-type doping levels in the emitter layer.

Figure 6. External quantum efficiency, internal quantum efficiency, and near-normal reflectance of GaInAsSb/AlGaAsSb/TPV cell.

Figure 7. Open-circuit voltage vs. short-circuit current density of 0.53-eV GaInAsSb/AlGaAsSb/GaSb TPV cell at room temperature.

Figure 8. Internal quantum efficiency of GaInAsSb/(AlGaAsSb)/GaSb TPV cells with various cutoff wavelength.

Figure 9. Voltage factor vs. energy gap of GaSb [17], GaInAsSb, and InPAsSb [25] TPV cells.

Figure 10. Inverse PL lifetime versus inverse GaInAsSb thickness of GaInAsSb/AlGaAsSb double heterostructures: (¦) GaSb capping layers; (?) Al content of AlGaAsSb is 0.2; (?) Al content of AlGaAsSb is 0.25.

Figure 11. Schematic structure of wafer-bonded GaInAsSb TPV cells with monolithic interconnections on a SI GaAs handle wafer.

Figure 12. Semi-logarithmic plot of J_{sc} versus V_{oc} for one-junction, two-junction, and ten-junction wafer-bonded TPV GaInAsSb devices.

Table 1. Device results of 0.53-eV GaInAsSb/AlGaAsSb/GaSb TPV cells.

Run no.	Doping level ($x10^{17}$ cm^{-3})	I_s (x 10^{-5} A)	R_s (x 10^{-3} ohm)	V_{oc} @ 3 A/cm^2 (mV)	FF (%)
99-18	1	1.5	8.2	316	68.0
99-15	2	1.8	6.4	320	68.9
99-16	4	0.95	4.9	319	70.8
99-17	10	1.12	3.6	321	70.9

Figure 1

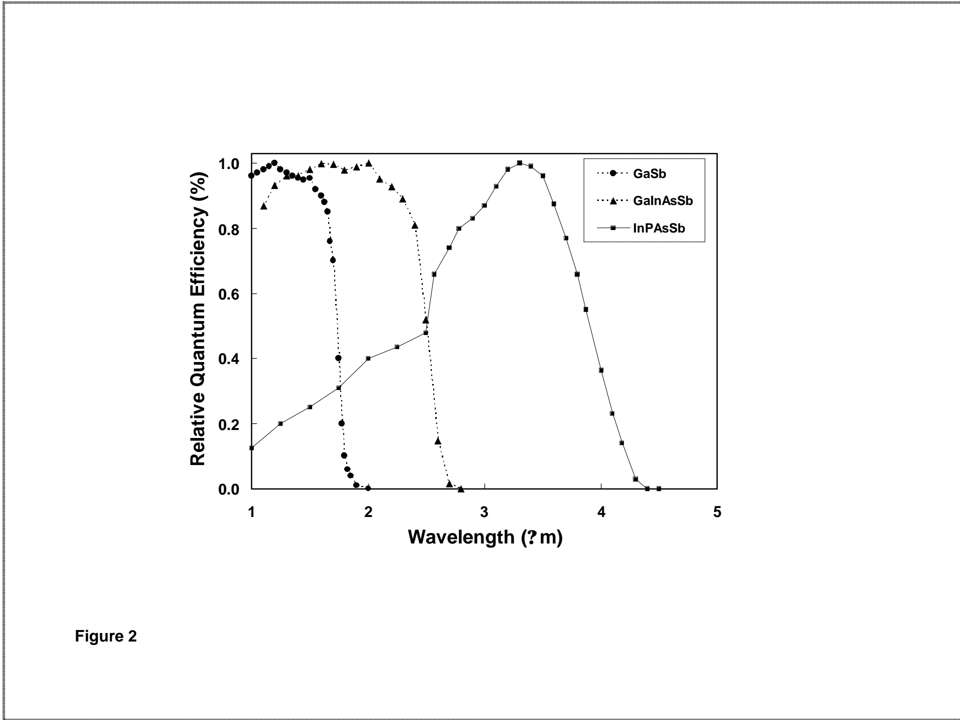

Figure 2

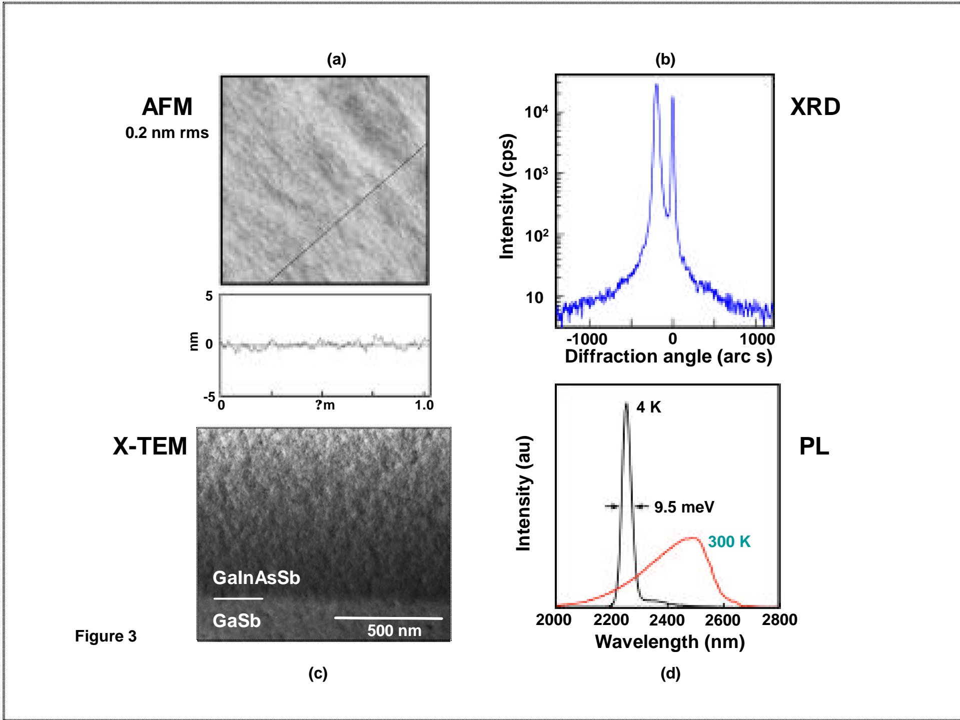

Figure 3

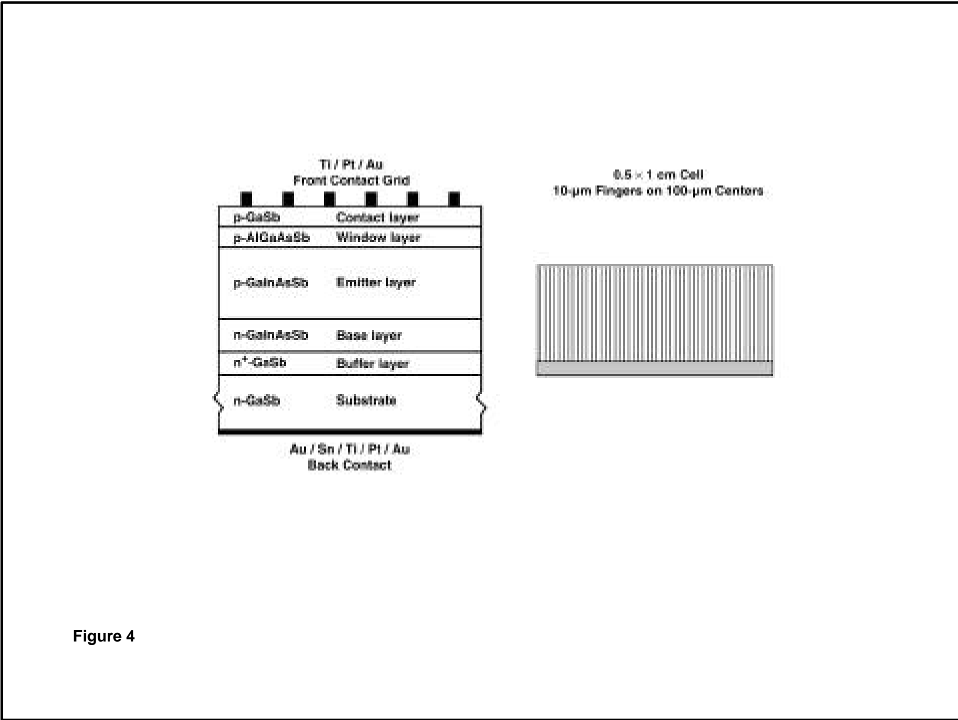

Figure 4

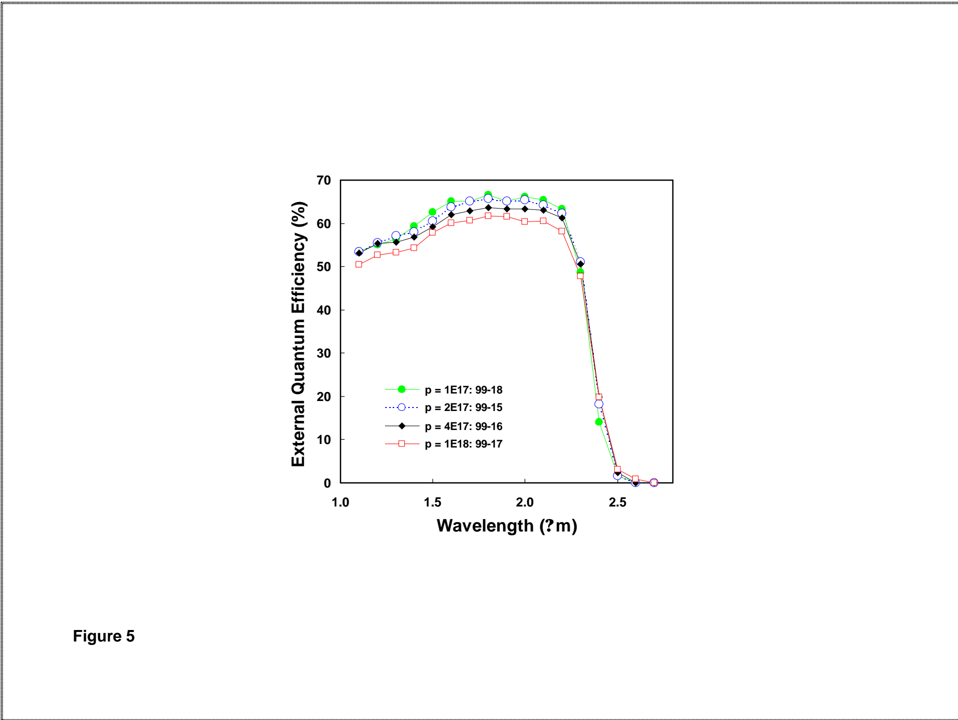

Figure 5

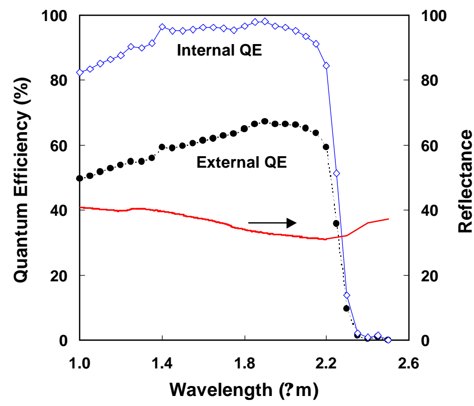

Figure 6

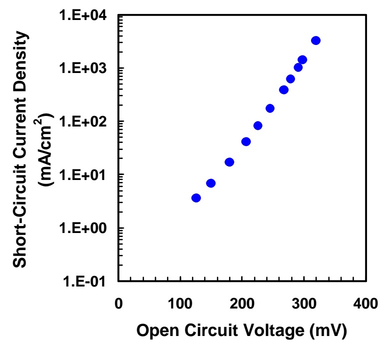

Figure 7

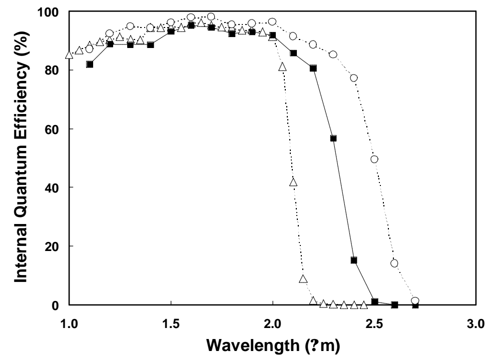

Figure 8

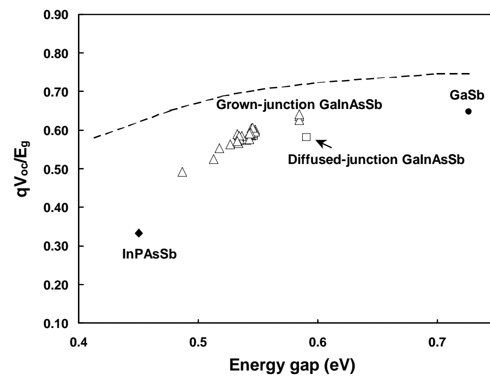

Figure 9

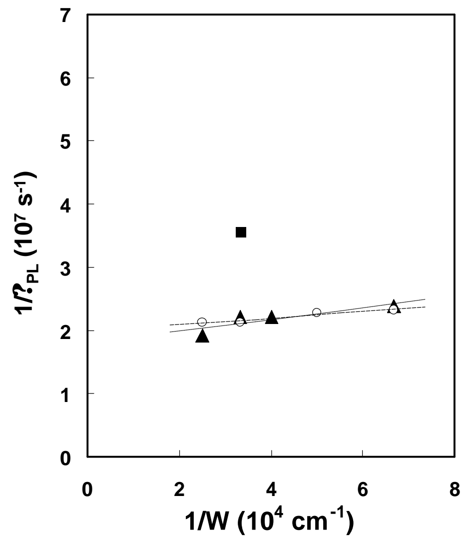

Figure 10

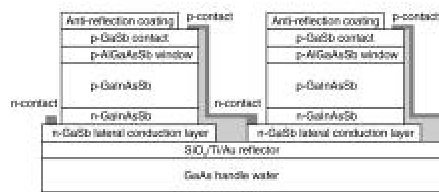

Figure 11

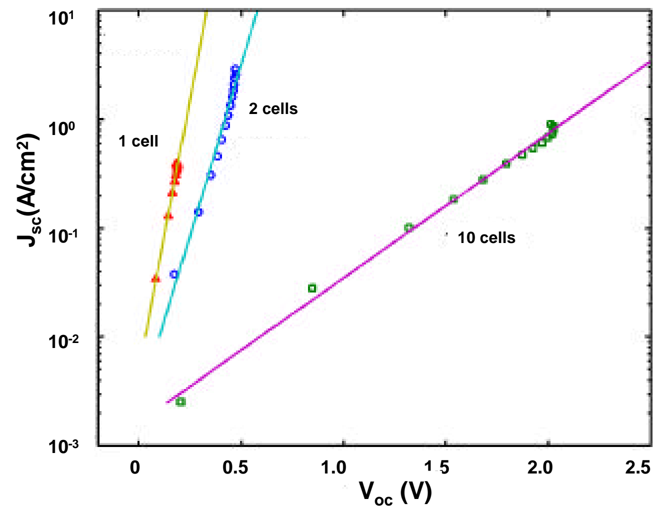

Figure 12